SIMULATION OF CONTROL OF THERMAL CONVECTION USING EXTERNAL MAGNETIC FIELD WITH DIFFERENT ORIENTATION AND DISTRIBUTION

S. Kenjereš and K. Hanjalić
Department of Multiscale Physics, Faculty of Applied Physics,
Delft University of Technology
Lorentzweg 1, 2628 CJ Delft, The Netherlands
kenjeres@ws.tn.tudelft.nl, hanjalic@ws.tn.tudelft.nl

ABSTRACT

We report on numerical study of effects of orientation and distribution of an external magnetic field on the reorganization of convective structures and heat transfer in thermal convection in electrically conductive fluids. The simulations were performed using a transient RANS (T-RANS) approach in which the large-scale deterministic structures are numerically resolved in time and space and the unresolved contribution is modelled using an algebraic stress-flux three-equation subscale model. For low Prandtl (Pr) fluids the subscale model was extended by including Pr-dependent molecular dissipation of heat flux, which lead to excellent agreement with DNS results for low-Pr classical Rayleigh-Bénard (RB) convection. The T-RANS approach, tested earlier in a number of cases of thermal and magnetic convection, was first applied to natural convection in a side-heated cubical enclosure subjected to magnetic field of different orientation, strength and depth, showing good agreement with previous benchmark studies. Then, a series of simulations was performed of turbulent RB convection subjected to different magnetic fields over a range of Rayleigh (Ra) and Hartmann (Ha) numbers. The computed Nusselt number showed good agreement with the available experimental results. Numerical visualization of instantaneous flow pattern reveals dramatic differences in the convective structures and local heat transfer for different orientation of the magnetic field with respect to the gravitation vector. It was found that a local magnetic field confined to the wall boundary layer along the thermally active walls provides almost equal effects as the homogeneous field over the whole flow, indicating an interesting possibility for controlling thermal convection and associated heat transfer.

INTRODUCTION

The potential of using a magnetic field to control fluid flow and heat transfer in conductive fluids has long been recognized in many applications such as crystal growth, continuous metal casting, liquid metal cooling blankets for fusion reactors, and others. An imposed magnetic field on electrically conducting fluid leads to the Lorentz force in the plane perpendicular to the magnetic field vector, oriented in the direction opposite to the fluid velocity in that plane, thus retarding the motion perpendicular to the magnetic field. A number of numerical and experimental studies of thermal convection subjected to magnetic field of various orientation have been reported in the literature, but most deal with laminar flows, e.g. Ozoe and Okada (1989), Mößner and Müller (1999), Juel *et al.* (1999). If the flow is turbulent, turbulence becomes suppressed, but much more anisotropic, approaching the one-component limit. The effect of combined thermal buoyancy and Lorentz force on turbulence, and particularly on its structure morphology, depends on the mutual orientation between the two body forces. Capturing these effects at higher Re and Ra numbers and in complex geometries, which are beyond the capability of direct numerical simulation (Rucklidge *et al.*, 2000), requires to model the magnetic effects on turbulence either for the full spectrum as in RANS or at least for the subscale turbulence for LES and VLES approaches. We consider different combinations, i.e. situations where the Lorentz force is aligned or perpendicular to the gravitational vector, both for a range of Ha and Ra numbers. The imposed magnetic fields are either homogeneously distributed over the whole flow domain, or locally confined to affect only the thin boundary layers along the thermally active walls.

EQUATIONS AND THE 'SUBSCALE MODEL'

We have applied transient RANS approach (T-RANS) which was extensively tested earlier in classical Rayleigh-Bénard convection over horizontal flat and wavy surfaces over a range of Ra numbers, $10^4 \leq Ra \leq 10^{15}$, all resulting in very good agreement with the available DNS and experimental results. This approach can be regarded as Very Large Eddy Simulations (VLES) in which the unresolved random motion is modeled using a $\langle k\rangle - \langle\varepsilon\rangle - \langle\theta^2\rangle$ algebraic stress/flux single-point closure models, Hanjalić and Kenjereš (2001). In contrast to LES, the contribution of both modes (resolved and subscale) to the turbulent fluctuations are of the same order of magnitude. The numerical method is then extended to include additional effects of magnetic fields and the integrated version of the Navier-Stokes-Maxwell's solver is developed. In addition to including the Lorentz force in the momentum equations

$$F_i^T = F_i^B + F_i^L = \beta g_i \left(\langle T\rangle - T_{REF}\right) + \frac{\sigma}{\rho}\left(-\epsilon_{ijk}\langle B_k\rangle \frac{\partial\langle\Phi\rangle}{\partial x_j} + \langle U_k\rangle\langle B_i\rangle\langle B_k\rangle - \langle U_i\rangle\langle B_k^2\rangle\right) \quad (1)$$

the influence of the magnetic field is taken into account by additional terms for subscale contributions to the turbulence kinetic energy $\langle k\rangle$ and its dissipation rate $\langle\varepsilon\rangle$, Kenjereš and Hanjalić (2000), Hanjalić and Kenjereš (2001):

$$G_k^L = -\frac{\sigma}{\rho} B_0^2 \langle k\rangle exp\left(-C_L \frac{\sigma}{\rho} B_0^2 \frac{\langle k\rangle}{\langle\varepsilon\rangle}\right), G_\varepsilon^L = C_{\varepsilon 4}\, G_k^L \frac{\langle\varepsilon\rangle}{\langle k\rangle} \quad (2)$$

with C_L=0.025 and $C_{\varepsilon 4}$=1. The subscale contribution to the turbulent heat flux is expressed in the following form:

$$\tau_{\theta i} = -C_\phi \frac{\langle k\rangle}{\langle\varepsilon\rangle}\left[\tau_{ij}\frac{\partial\langle T\rangle}{\partial x_j} + \xi\tau_{\theta j}\frac{\partial\langle U_i\rangle}{\partial x_j} + \eta\left(\beta g_i\langle\theta^2\rangle + \langle\theta f_i^L\rangle\right) + \langle\varepsilon_{\theta i}\rangle\right] \quad (3)$$

where

$$f_i^L = \mathbf{j}\times\mathbf{B} = \frac{\sigma}{\rho}(\underbrace{-\nabla\phi_e + \mathbf{u}\times\mathbf{B}}_{\mathbf{e}})\times\mathbf{B}$$

$$\langle\varepsilon_{\theta i}\rangle = f_{\varepsilon_{\theta i}}\frac{1+Pr}{2\sqrt{PrR}}\frac{\langle\varepsilon\rangle}{\langle k\rangle}\tau_{\theta i} \quad (4)$$

are the fluctuating Lorentz force and the molecular heat flux dissipation, respectively.

SOLUTION METHOD

The equation set is solved using a finite-volume Navier-Stokes-Maxwell solver for three-dimensional flows in structured non-orthogonal geometries. The Cartesian vectors and tensors components and a colocated arrangements are applied for all variables. The second-order central difference scheme (CDS) is applied for the discretization of diffusive terms in all equations and of convective terms in $\langle U, V, W, T, \Phi \rangle$ equations. The second-order linear upwind scheme (LUDS) is applied for convective terms in equations of sub-scale turbulent contributions, i.e. $\langle k, \varepsilon, \theta^2 \rangle$. The time integration is performed by fully implicit second-order three-time-level method which allows larger time steps to be used (compared to explicit marching schemes).

RESULTS AND DISCUSSION

Natural convection in the side-heated cubical enclosure: laminar and transitional regimes

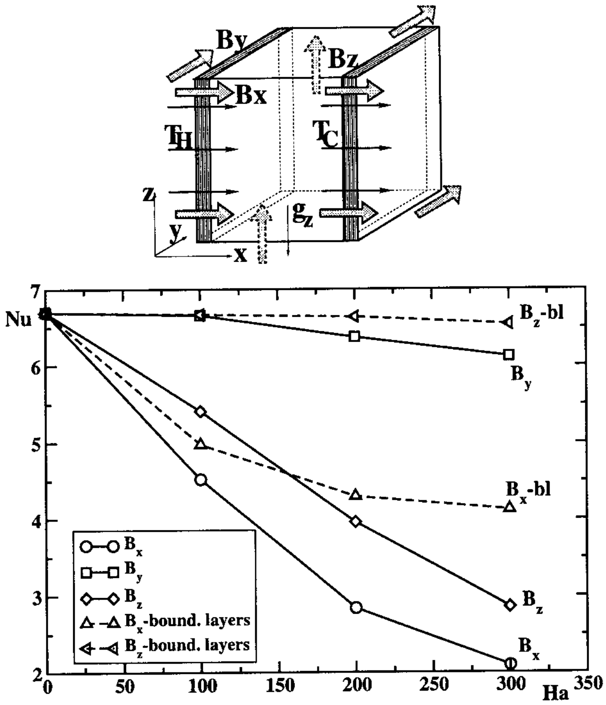

Figure 1: Reduction in the integral heat transfer coefficient for a side-heated cubical cavity subjected to external magnetic fields of different orientation distributed homogeneously or confined only to boundary layers along the thermally active vertical walls, B_x^{BL} and B_z^{BL}: $Ra=10^6$, $Pr=0.054$, $0 \leq Ha \leq 300$;

In order to validate the integrated Navier-Stokes - Maxwell solver, the three-dimensional numerical computations of magnetic laminar and transitional convection in electrically insulated cubical enclosure are performed and compared with similar simulations of Ozoe and Okada (1989), Mößner and Müller (1999) and Juel *et al.* (1999), yielding generally good agreement. It is observed that the maximum reduction in heat transfer is achieved when the magnetic field is imposed in the x-direction ($\mathbf{B}||x$), Fig.1. For the $\mathbf{B}||y$ orientation, only small changes in the reorganization of the flow structures are observes compared to the situations when the magnetic field is switched off, Fig.2. Consequently, very modest reductions of Nu are obtained even for the high values of Ha.

In addition to the homogeneously applied magnetic fields along the main coordinate directions, we also applied locally confined magnetic field which influences only the boundary layers along the thermally active walls. Here the magnetic field is active only in the near-wall region up to the distance where the vertical velocity in the situation when the magnetic field is switched off, reaches its maximum. The orientations of magnetic fields are chosen to be in the x- and z-direction since these orientations showed to be most efficient in damping the heat transfer. A strong reduction in heat transfer is again observed for $\mathbf{B}||x$ orientation. This damping of heat transfer for $0 \leq Ha \leq 150$ is even more efficient than $\mathbf{B}||z$ orientation applied along full distance. For $Ha \geq 200$ a further increase in the intensity of the magnetic field does not bring any significant reduction in Nu, i.e. a sort of an asymptotic state is approached. It is noted that this boundary-layer-confined magnetic field produced very significant reduction in heat transfer - about 40%. Such confined magnetic fields can easily be generated in practical applications and are considered as an attractive means for suppressing heat transfer. Note that a nonuniform mesh with 82^3 and 102^3 control cells clustered towards the walls has been applied for the homogeneously and partially imposed magnetic fields, respectively, ensuring in both cases that the Hartmann boundary layers ($\delta_H \propto 1/Ha$) are well resolved for all values of Ha.

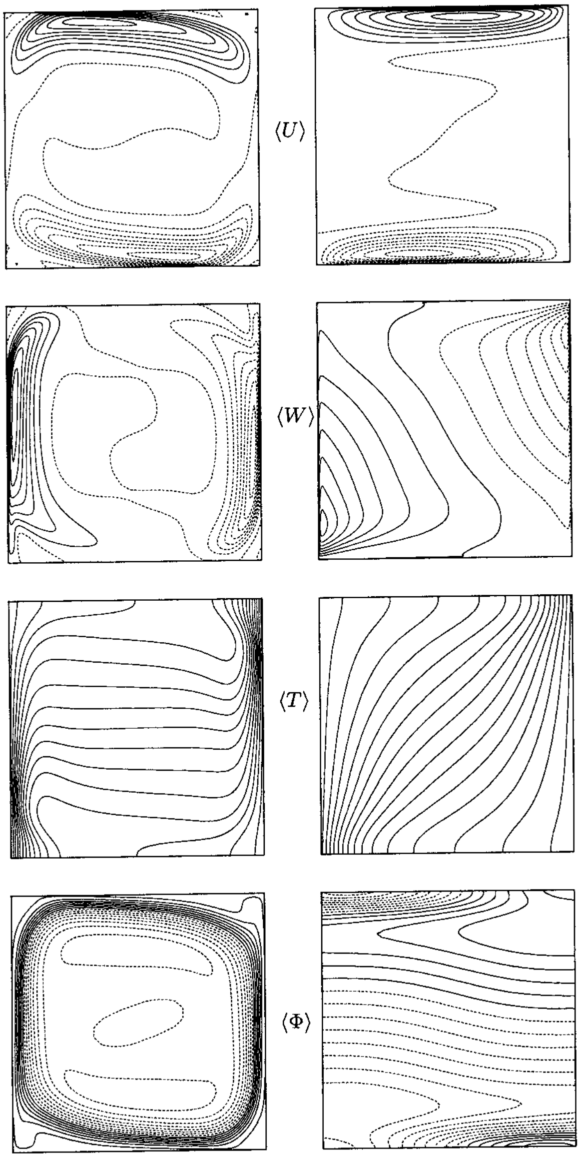

Figure 2: Reorganization of the flow pattern, temperature and electric potential fields in the central vertical (x-z) plane of a cubical cavity for different orientation of magnetic fields: left- $\mathbf{B}||y$, Ha=100, right- $\mathbf{B}||x$, Ha=300; $Ra=10^6$, $Pr=0.054$.

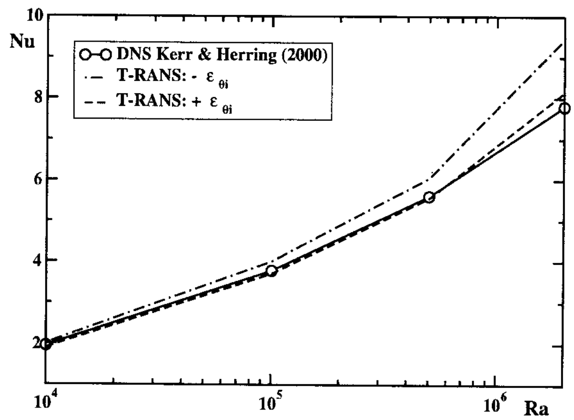

Figure 3: Effect of inclusion of the molecular heat flux dissipation $\langle\varepsilon_{\theta i}\rangle$ into subscale representation of turbulent heat flux $\tau_{\theta i}$: comparison with DNS results of Kerr and Herring (2000), $10^4 \leq Ra \leq 2\times10^6$, $Pr=0.07$.

Accounting for low Prandtl numbers

In our previous studies, Kenjereš and Hanjalić (2000) and Hanjalić and Kenjereš (2001), we presented a three-equations $\langle k\rangle-\langle\varepsilon\rangle-\langle\theta^2\rangle$ ASM/AFM model for turbulent flows simultaneously subjected to thermal buoyancy and Lorentz force, but considered only the fluids with the Prandtl number close to unity. Here we consider mostly liquid metals and introduce additional low-Pr modifications. In a series of direct numerical simulation (DNS) of RB convection with liquid metals (Pr=0.006, 0.025) Wörner and Grötzbach (1995) showed that the molecular destruction $\langle\varepsilon_{\theta i}\rangle$ was the main sink in the turbulent heat flux equation. Based on *a priori* test, they proposed a model which explicitly accounts for the Pr modifications, Eq.4, with

$$f_{\varepsilon\theta i} = exp\left[-C_{\varepsilon_{\theta i}} Re_t \left(1 + Pr\right)\right] \qquad (5)$$

where $Re_t=\langle k\rangle^2/\nu\langle\varepsilon\rangle$ is the Reynolds turbulent number and $C_{\varepsilon_{\theta i}}=7\times10^{-4}$. We applied this model to the computation of a classical low-Pr turbulent RB convection and compared results with recent DNS of Kerr and Herring (2000), $10^4 \leq Ra \leq 2\times10^6$, Pr=0.07. It can be seen that the inclusion of the $\langle\varepsilon_{\theta i}\rangle$ into $\tau_{\theta i}$ provided Nu in excellent agreement with DNS over the entire range of Ra, Fig. 3. It is noted that the computational mesh $82\times82\times72$ used here for T-RANS over a range of Ra numbers up to 2×10^{16} is much coarser than the DNS mesh $256\times256\times128$ for DNS used by Kerr for $Ra=2\times10^6$.

Magnetic turbulent thermal convection

Next, we consider thermal convection subjected to external magnetic fields of different orientations over a range of Ra ($10^7 \leq Ra \leq 10^9$) and Ha ($0 \leq Ha \leq 500$). The effect of a transversal magnetic field ($\mathbf{B}||z$) on integral heat transfer (Nu) for all simulated situations is shown in Fig.4. Good agreement between the present simulations and experimental results of Cioni *et al.* (2000) have been obtained despite the difference in geometries considered: the experiments were performed in a vertical cylinder with aspect ratio $D/H=1$ where one may expect more intensive convection compared to the classical RB between infinite walls. It is noted that for all Ra numbers considered, the flow will be highly turbulent in the absence of the magnetic field. As expected, very significant reduction in heat transfer is observed. With this orientation of magnetic field, it is even possible to totally suppress any convective motion and to produce pure diffusive regime. This effect can be easily explained since the vertically oriented magnetic field creates Lorentz force which acts in the horizontal plane and suppresses horizontal motion creating vertically elongated convective cell pattern, with very thin thermal plumes in between, Fig.5. With an increase in the intensity of the magnetic

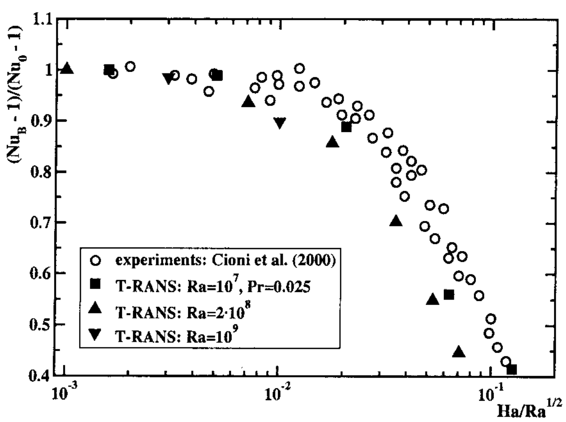

Figure 4: Reduction in the integral heat transfer coefficient for highly turbulent Rayleigh-Bénard convection subjected to a vertical magnetic field of different intensity $10^7 \leq Ra \leq 10^9$, $0<Ha \leq 500$, Pr=0.025 - comparison with experimental results of Cioni *et al.* (2000).

field these structures are 'squeezed' further until they break and the entire convective motion will be totally suppressed.

The reorganization of the vertical velocity $\langle W\rangle$ and temperature $\langle T\rangle$ in the central vertical plane for different orientations of magnetic field is illustrated in Fig. 6. For $\mathbf{B}||z$ situation where the magnetic field is locally confined to the near-wall regions ($0 \leq z/D \leq 0.005$, $0.95 \leq z/D \leq 1$), the structure gets detached from the wall boundary layers, levitating freely in the core region. The locally applied magnetic field near the walls almost totally suppresses the velocity and its fluctuations in this region, creating conductive-like buffer with almost linear distribution of temperature field, Fig. 6-middle. This finding can be of use for controlling heat transfer in various applications, such as future generation of fusion reactors. In addition, in the central zone the temperature contours show less pronounced gradients indicating a better mixing. With longitudinal orientation of homogeneously distributed magnetic field ($\mathbf{B}||y$) significantly different picture is obtained, Fig. 6-bottom. Very regular, two-dimensional morphology of velocity and temperature field is observed. This is in accordance with our expectations since this configuration should produce structures elongated in direction of applied magnetic field. It is interesting to notice the additional small cells nested just below/above the large rolls with rotation in the opposite direction, Fig. 6-bottom.

In order to quantify the effects of flow structure reorganizations on integral heat transfer (for this specific value of $Ra=10^7$), the Nu dependence on Ha is shown in Fig.7. It is already mentioned that for a homogeneously distributed magnetic field, the $\mathbf{B}||z$ orientation is can lead to the pure diffusive regime. In contrast to this situation, the $\mathbf{B}||y$ orientation reduces significantly heat transfer until the point that the fully two-dimensional state is obtained. After this point, additional increase in magnetic field intensity will not bring any additional heat transfer reduction. Interesting behavior of $Nu-Ha$ dependence can be observed for different situations. For the weak magnetic fields, $15 \leq Ha \leq 65$, the $\mathbf{B}||y$ orientation resulted in the weakest heat transfer reduction. In the $65 \leq Ha \leq 200$ interval, due to very dramatic flow reorganization towards the two-dimensional state, heat transfer is reduced much more efficiently than in the case of partially confined $\mathbf{B}||z$ orientation. In the same interval, a very strong damping of Nu occurs for the locally confined $\mathbf{B}||z$ orientation. It can be concluded that for all considered situations a highly non-monotonic behavior is observed. This finding stresses the importance of the distributions of the imposed magnetic field and its orientation with respect to the gravitational vector in controlling heat transfer.

A further illustration of the flow reorganization due to an imposed magnetic field is given by plots of the contours of the instanta-

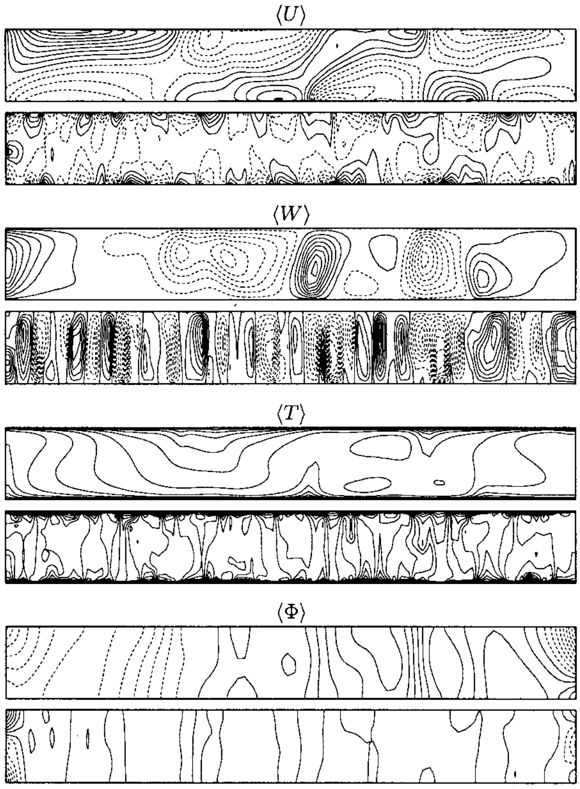

Figure 5: Rayleigh-Bénard turbulent convection subjected to a vertically oriented magnetic field: Ra=2×10^8, Pr=0.025, first- Ha=100, second- Ha=500: from above to bellow: distribution of instantaneous horizontal $\langle U \rangle$, vertical velocity $\langle W \rangle$, temperature $\langle T \rangle$ and electric potential $\langle \Phi \rangle$ in the central vertical cross-section.

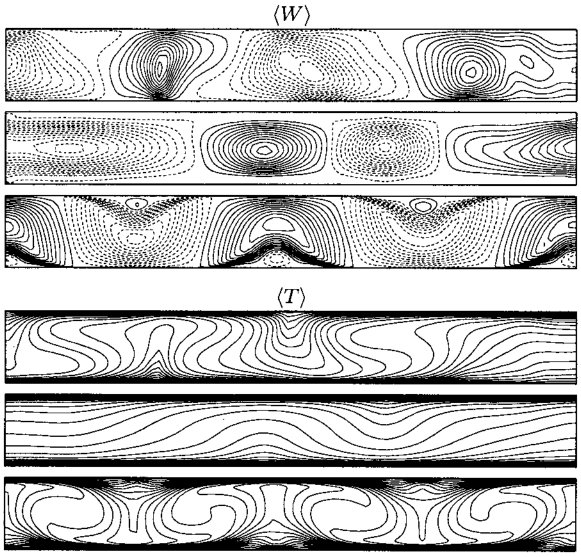

Figure 6: Turbulent Rayleigh-Bénard convection (Ra=10^7, Pr=0.025) subjected to external magnetic fields of different orientation and strength: first- Ha=0; second- Ha=500, vertical magnetic field applied in the near wall region $0 \le z/D < 0.05$ and $0.95 \le z/D < 1$; third - longitudinal magnetic field, Ha=500.

neous vertical velocity and temperature in the central horizontal plane, Figs.8,9. Compared to the neutral situation (Ha=0), both $\mathbf{B}||z$ and $\mathbf{B}||y$ orientations at Ha=200 produced dramatic changes in flow and temperature fields. In principle, two basic trends can be seen:

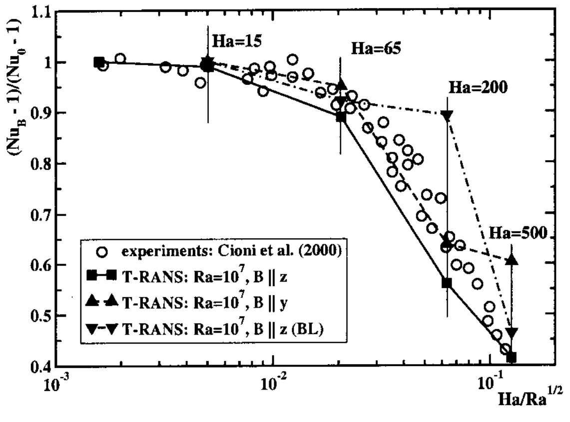

Figure 7: Effects of different magnetic field orientations on integral heat transfer, Ra=10^7, Pr=0.025.

the $\mathbf{B}||z$ orientation tends to produce more dense structures (damping of convective structures) and the $\mathbf{B}||y$ orientation tends to impose two-dimensional alignments in the y-direction. The imprints of the underlying thermal plumes and produced up- and down-drafts can be seen in Fig. 8. Here, the contours of positive or negative values of $\langle W \rangle$ are plotted with solid and dashed lines respectively. As expected, very close resemblance between the thermal and velocity field is observed, Fig. 9.

A summary of local distributions of Nu at the hot wall for considered test cases is shown in Fig. 10. It is interesting to observe that the $\mathbf{B}||z$ orientation can produce larger local values of Nu compared to the neutral situations (Ha=0) despite the fact that the integral heat transfer is reduced. This can be explained by more intensive penetrative capabilities of the vertically elongated nearly cylindrical thermal plumes which produce stronger local temperature gradients. The effects of the $\mathbf{B}||y$ orientation show gradually appearing alignment with the y-axis. For the most intensive magnetic field applied (Ha=500) very regular two-dimensional sinusoidal distributions is obtained. It is already mentioned that the locally confined $\mathbf{B}||z$ orientation produced very rapid damping of Nu. At the same time a quite uniform distribution of the local Nu.

CONCLUSIONS

The time-dependent Reynolds-averaged Navier-Stokes method (T-RANS), tested earlier in various flows dominated by large-scale deterministic structures, was applied to study effects of different distribution and orientation of an imposed magnetic field on flow and heat transfer in thermal convection. Two configurations were considered: a side-heated cavity and Rayleigh-Bénard convection, both for a range of Ra and Ha numbers. The computed convective structures and Nusselt number distribution on the bounding horizontal walls reveal very different effects of the imposed magnetic field depending on its orientation and distribution. For a side-heated cavity, the horizontal magnetic field ($\mathbf{B}||x$) aligned with the mean temperature gradient (∇T) produces a drastic heat transfer damping, whereas the spanwise horizontal field ($\mathbf{B}||y$, perpendicular to ∇T) causes hardly any changes. In the case of RB convection, a vertical homogenous magnetic field causes a strong reduction in both the integral and local heat transfer coefficients, while in a spanwise field the effect is much weaker.

The application of a local wall-normal magnetic field, confined to the near-wall region, proved in both configurations to be almost equally effective as the homogeneous field over the entire flow, especially for lower magnetic intensities. Because a local magnetic field in the near-wall region can easily be generated in practical situations, this finding opens an interesting potential for controlling heat transfer

Figure 8: Vertical velocity $\langle W \rangle$ distribution in the central horizontal plane (z/D=0.5), Ra=10^7, Pr=0.025: first- Ha=0, no magnetic field; second- Ha=200, transversal magnetic field ($\mathbf{B}||z$) ; third- Ha=200, longitudinal magnetic field ($\mathbf{B}||y$).

in thermal convection.

The T-RANS approach was demonstrated to be a credible tool for optimization of magnetic field to control heat transfer in various applications.

ACKNOWLEDGMENT

The research of Dr. Saša Kenjereš has been made possible by a fellowship of the Royal Netherlands Academy of Arts and Sciences (KNAW).

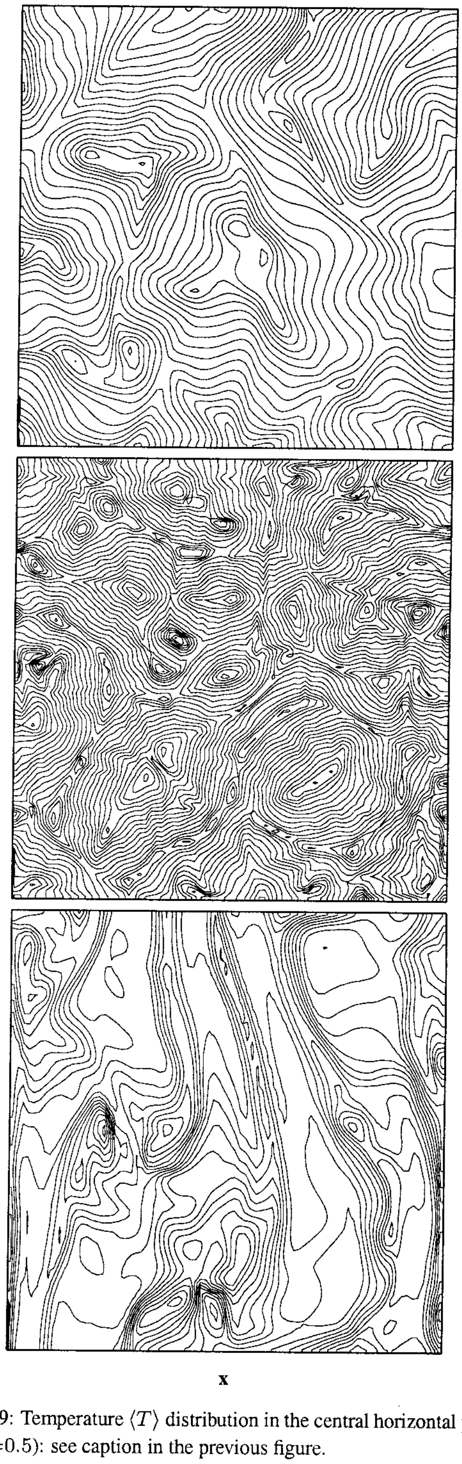

Figure 9: Temperature $\langle T \rangle$ distribution in the central horizontal plane (z/D=0.5): see caption in the previous figure.

REFERENCES

Berger T., Kim J., Lee C. and Lim J., (2000), "Turbulent boundary layer control utilizing the Lorentz force", *Phys. of Fluids*, Vol.12, No.3, pp. 631-649.

Burr U. and Müller U., (2001), "Rayleigh-Bénard convection in liquid metal layers under the influence of a vertical magnetic field", *Phys. of Fluids*, Vol.13, No.11, pp. 3247-3257.

Cioni S., Chaumat S. and Sommeria J., (2000), "Effect of a vertical magnetic field on turbulent Rayleigh-Bénard convection", *Phys. Review E*, Vol.62, No.4, pp. 4520-4523.

Hanjalić K. and Kenjereš S, (2001), "T-RANS Simulation of Deterministic Eddy Structure in Flows Driven by Thermal Buoyancy and

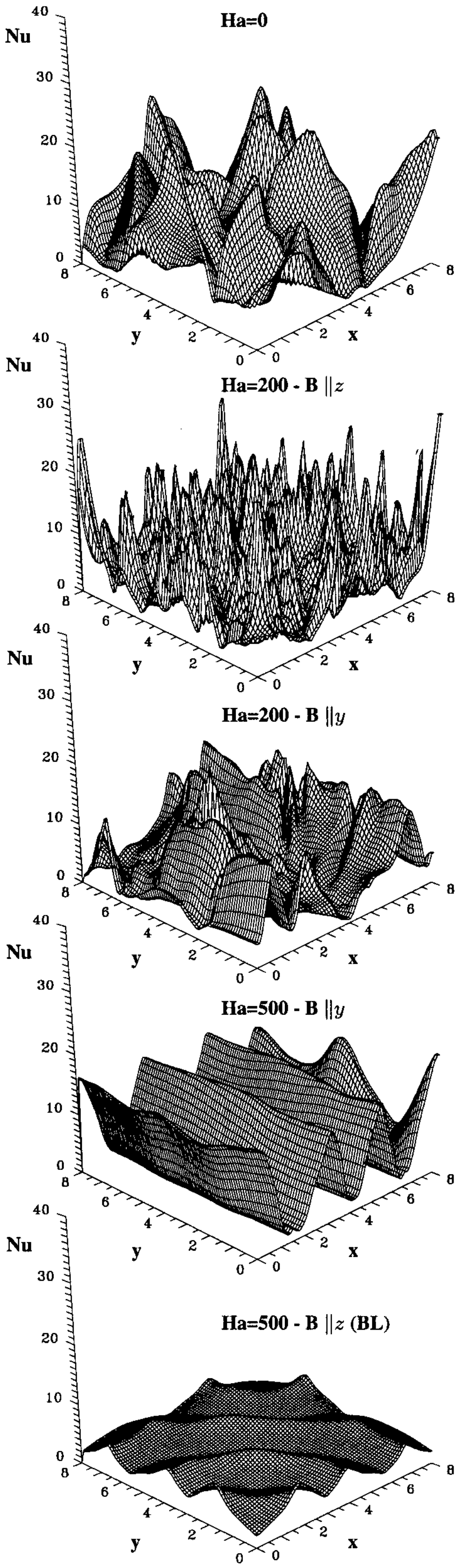

Figure 10: Distributions of the local Nusselt number on the hot wall for different orientations, distributions and intensities of external magnetic field: Ra=10^7, Pr=0.025.

Lorentz Force", *Flow, Turbulence and Combustion*, Vol.66, pp. 427-451.

Juel A., Mullin T., Ben Hadid H. and Henry D., (1999), "Magnetohydrodynamic convection in molten gallium", *J. Fluid Mechanics*, Vol.378, pp. 97-118.

Kenjereš S. and Hanjalić K., (2000), "On the implementation of effects of Lorentz force in turbulence closure models", *Int. J. Heat and Fluid Flow*, Vol.21 (3), pp. 329-337.

Kerr R. M. and Herring J. R., (2000) "Prandtl number dependence of Nusselt number in direct numerical simulations", *J. Fluid Mechanics*, Vol.419, pp. 325-344.

Mößner R. and Müller U., (1999), "A numerical investigation of three-dimensional magneto-convection in rectangular cavities", *Int. J. Heat and Mass Transfer*, Vol.42, pp. 1111-1121.

Ozoe H. and Okada K., (1989), "The effect of the direction of the external magnetic field on the three-dimensional natural convection in a cubical enclosure", *Int. J. Heat and Mass Transfer*, Vol.32, pp. 1939-1954.

Rucklidge A. M., Weiss N. O., Brownjohn D. P., Matthews P. C. and Proctor M. R. E., (2000), "Compressible magneto-convection in three dimensions: pattern formation in a strongly stratified layer", *J. Fluid Mechanics*, Vol.419, pp.283-323.

Wörner M. and Grötzbach G., (1995), "Modeling the molecular terms in the turbulent heat flux equation for natural convection", *10th Symposium on Turbulent Shear Flows*, Vol.2, pp.73-78, Pennsylvania State University, State Colege, U.S.A.